

Metadata of the article that will be visualized in OnlineFirst

1	Article Title	Carbon and Water Exchanges in a Mountain Meadow Ecosystem, Sierra Nevada, California
2	Article Sub- Title	
3	Article Copyright - Year	Society of Wetland Scientists 2021 (This will be the copyright line in the final PDF)
4	Journal Name	Wetlands
5	Family Name	Oliphant
6	Particle	
7	Given Name	Andrew J.
8	Corresponding	Suffix
9	Author	Organization San Francisco State University
10		Division Department of Geography & Environment
11		Address San Francisco, California, USA
12		e-mail andrewo@sfsu.edu
13	Family Name	Blackburn
14	Particle	
15	Given Name	Darren A.
16	Suffix	
17	Author	Organization San Francisco State University
18		Division Department of Geography & Environment
19		Address San Francisco, California, USA
20		e-mail
21	Family Name	Davis
22	Particle	
23	Given Name	Jerry D.
24	Author	Suffix
25		Organization San Francisco State University
26		Division Department of Geography & Environment
27		Address San Francisco, California, USA
28		e-mail
29	Received	9 February 2020
30	Schedule	Revised
31		Accepted 26 February 2021

32	Abstract	<p>Ecosystem-atmosphere exchanges of carbon dioxide (CO_2) and water vapor were investigated in a moist mountain meadow (Loney Meadow) at 1822 m MSL in the Sierra Nevada, California, USA. An eddy covariance (EC) tower was deployed for most of the snow-free period from May to September 2016. The meadow ecosystem progressed from a strong sink of CO_2 in the peak of the growing season under saturated to wet soil conditions ($-18.51 \text{ gC m}^{-2} \text{ d}^{-1}$) to a weak source ($2.97 \text{ gC m}^{-2} \text{ d}^{-1}$) following a rapid decline in soil moisture as runoff decreased. The variability of Net Ecosystem Exchange (NEE) over diurnal, synoptic and seasonal timescales was dominated by Gross Primary Production (GPP) which ranged from $43 \text{ gC m}^{-2} \text{ d}^{-1}$ during the peak of the growing season to $19 \text{ gC m}^{-2} \text{ d}^{-1}$ during senescence. Ecosystem respiration was small in magnitude and variability compared to GPP. Approximations of annual NEE for the meadow ranged from -285 to $-450 \text{ gC m}^{-2} \text{ yr}^{-1}$, which is high compared to grasslands, and more similar to mature wetland or forest ecosystems. At diurnal and synoptic scales, CO_2 flux was driven most strongly by photosynthetically active radiation (PAR), while seasonally, the ecosystem was linked closely to changes in soil moisture. Light-use and water-use efficiencies of the meadow ecosystem were high compared with those found in most other ecosystems using comparable observations. These results suggest meadows have the potential to be large sinks of atmospheric CO_2 and that their ability to do so is sensitive to water table height. This is important for understanding the future of carbon sequestration in mountain meadows in the context of changing hydroclimates and different land management decisions that impact meadow hydrology.</p>
33	Keywords separated by '-'	Mountain meadow - Carbon cycle - Evapotranspiration - Biometeorology, ecosystems
34	Foot note information	<p>This article is part of the Topical Collection on <i>Wetlands and Global change</i> Springer Nature remains neutral with regard to jurisdictional claims in published maps and institutional affiliations.</p>

1
25
6
7

Carbon and Water Exchanges in a Mountain Meadow Ecosystem, Sierra Nevada, California

8 Darren A. Blackburn¹ · Andrew J. Oliphant¹ · Jerry D. Davis¹
9

10 Received: 9 February 2020 / Accepted: 26 February 2021

11 © Society of Wetland Scientists 2021

12

Abstract

Ecosystem-atmosphere exchanges of carbon dioxide (CO_2) and water vapor were investigated in a moist mountain meadow (Loney Meadow) at 1822 m MSL in the Sierra Nevada, California, USA. An eddy covariance (EC) tower was deployed for most of the snow-free period from May to September 2016. The meadow ecosystem progressed from a strong sink of CO_2 in the peak of the growing season under saturated to wet soil conditions ($-18.51 \text{ gC m}^{-2} \text{ d}^{-1}$) to a weak source ($2.97 \text{ gC m}^{-2} \text{ d}^{-1}$) following a rapid decline in soil moisture as runoff decreased. The variability of Net Ecosystem Exchange (NEE) over diurnal, synoptic and seasonal timescales was dominated by Gross Primary Production (GPP) which ranged from $43 \text{ gC m}^{-2} \text{ d}^{-1}$ during the peak of the growing season to $19 \text{ gC m}^{-2} \text{ d}^{-1}$ during senescence. Ecosystem respiration was small in magnitude and variability compared to GPP . Approximations of annual NEE for the meadow ranged from -285 to $-450 \text{ gC m}^{-2} \text{ yr}^{-1}$, which is high compared to grasslands, and more similar to mature wetland or forest ecosystems. At diurnal and synoptic scales, CO_2 flux was driven most strongly by photosynthetically active radiation (PAR), while seasonally, the ecosystem was linked closely to changes in soil moisture. Light-use and water-use efficiencies of the meadow ecosystem were high compared with those found in most other ecosystems using comparable observations. These results suggest meadows have the potential to be large sinks of atmospheric CO_2 and that their ability to do so is sensitive to water table height. This is important for understanding the future of carbon sequestration in mountain meadows in the context of changing hydroclimates and different land management decisions that impact meadow hydrology.

28

Keywords Mountain meadow · Carbon cycle · Evapotranspiration · Biometeorology, ecosystems

29

Introduction

30
31
32
33
34
35
36
37
38

Mountain meadows are important environmental systems that form in topographical depressions and low-gradient valley bottoms, often containing shallow groundwater, finely textured and organically rich soils and abundant plants dominated by hydric to mesic herbaceous species. In the Sierra Nevada (SN) range of California and Nevada, USA, Viers et al. (2013) estimated that there were more than 17,000 meadows covering nearly 78,000 ha of land. Although they

account for a relatively small percentage of land cover (~0.01%), most tributaries pass through multiple sequences of meadows within SN watersheds, which have important water quality and discharge controls.

There is a significant amount of diversity among SN meadows resulting in a wide range of hydrogeomorphic types ranging from peatlands and depressions to more riparian systems (Weixelman et al. 2011). Hydrologic inputs to local meadow aquifers include springs from geologic aquifers, hill-slope runoff and surface streams (Loheide et al. 2009). Ecological and rangeland classifications are strongly influenced by hydrology, with wetland obligate or facultative plant assemblages dependent on water table depth and the amount of time water covers the meadow surface (Ratliff 1985; Allen 1987; Dwire et al. 2006). A shallow groundwater table sustaining high soil moisture levels through much of the growth period is the most important factor in maintaining the characteristic herbaceous communities found in wet meadows (Fites-Kaufman et al. 2007; Loheide et al. 2009). With

This article is part of the Topical Collection on *Wetlands and Global change*

✉ Andrew J. Oliphant
andrewo@sfsu.edu

¹ Department of Geography & Environment, San Francisco State University, San Francisco, California, USA

58 seasonal runoff influenced greatly by snowmelt, SN meadows
 59 produce strong seasonal hydrologic and ecologic cycles, be-
 60 having much like seasonal wetlands (Ratliff 1985; Loheide
 61 et al. 2009).

62 Vegetation in undegraded meadows typically consists of
 63 hydric and mesic species such as perennial grasses, wet
 64 sedges, forbs, and other herbaceous species (Ratliff 1985;
 65 Allen 1987; Lowry et al. 2011; Maher 2015). The spatial
 66 patterns of vegetation within individual meadows are indica-
 67 tive of an extensive land-water ecotone driven by soil mois-
 68 ture gradients (Kondolf et al. 1996).

69 Ecosystems in meadows with significant riparian and hill-
 70 slope water sources exhibit strong seasonality with annual
 71 growth cycles that begin in the late spring due to snowmelt-
 72 induced runoff, senesce from mid to late summer as water
 73 tables lower, and often snow covers meadow surfaces in win-
 74 ter (Loheide and Gorelick 2007). The timing of spring snow-
 75 melt, peak streamflow, snow cover and the relative seasonal
 76 snow water equivalent (SWE) in the SN are influenced by
 77 inter-annual and decadal-scale climate variability (Hamlet
 78 et al. 2005; Stewart et al. 2005). In general, over the past five
 79 decades, the timing of spring streamflow in western North
 80 America has been arriving earlier and with less precipitation
 81 falling as snow (Stewart et al. 2005; Lowry et al. 2011; Viers
 82 and Rheinheimer 2011). Previous studies of moist meadow
 83 carbon cycling have primarily focused on carbon stocks from
 84 biometric estimates (Norton et al. 2011; Reed et al. 2020) but
 85 much less is known about the rates of CO₂ exchange, its sea-
 86 sonal evolution and its main environmental controls (Fites-
 87 Kaufman et al. 2007).

88 Mountain meadows are also sensitive to land use changes
 89 and many of these ecological processes have been altered as a
 90 result of anthropogenic activities (Ratliff 1982; Kattelmann
 91 and Embury 1996; Purdy and Moyle 2006; Loheide and
 92 Gorelick 2007). Historic and current land use (e.g., grazing,
 93 logging and mining) in the Sierra Nevada have contributed to
 94 increased stream channel incision in riparian meadows (Ratliff
 95 1985; Kattelmann and Embury 1996; Purdy and Moyle 2006;
 96 Viers et al. 2013; Lowry et al. 2011; Weixelman et al. 2011).
 97 This channel incision can disconnect the stream channel from
 98 the meadow floodplain, lowering the water table and reducing
 99 soil water content in the root zone, which impacts the produc-
 100 tivity and distribution of native vegetation (Kattelmann and
 101 Embury 1996; Loheide et al. 2009; Lowry et al. 2011). Lowering
 102 of the water table also allows oxygenation of organically rich
 103 soil, which enhances soil microbial respiration resulting in the
 104 accelerated loss of stored soil carbon (Scott et al. 2010; Knox
 105 et al. 2015).

106 The impact of degradation on vegetation patterns tends to
 107 be a succession from native hydric/mesic species to more xe-
 108 ric species commonly associated with dryland meadows
 109 (Allen-Diaz 1991; Loheide and Gorelick 2007; Loheide
 110 et al. 2009; Pope et al. 2015). Previous studies have linked

111 water availability in meadows to fluctuations in species rich-
 112 ness, vulnerability to invasive species encroachment and the
 113 capacity to sequester atmospheric CO₂ for plant production
 114 and contribute to soil carbon storage (Dwire et al. 2006;
 115 Fites-Kaufman et al. 2007; Haugo and Halpern 2007;
 116 Blankinship and Hart 2014; Maher 2015). A comparison of
 117 existing measurements of CO₂ fluxes in wetland, grassland
 118 and semi-arid ecosystems suggests that hydric/mesic species
 119 are much faster growing and absorb greater amounts of CO₂
 120 from the atmosphere (e.g. Ratliff 1985; Flanagan et al. 2002;
 121 Kayranli et al. 2010; Norton et al. 2011). Xeric species, on the
 122 other hand, tend to be weak sinks of carbon and can shift from
 123 a net sink to a source of carbon dioxide to the atmosphere
 124 during dry years (Lund et al. 2010; Scott et al. 2010). Because
 125 of the important ecological benefits and services that
 126 mountain meadows provide, such as water quality and flood
 127 control, carbon sequestration and storage, biodiversity en-
 128 hancement, and culturally important food and weaving re-
 129 sources, there has been increased interest in restoring
 130 meadows that have been degraded due to anthropogenic ac-
 131 tivities (Loheide and Gorelick 2007; Pope et al. 2015). The
 132 goal of these “rewatering” projects is to mimic and restore
 133 natural processes that raise the volume of subsurface storage
 134 by providing a greater spatial opportunity for water to infil-
 135 trate (Hammersmark et al. 2008). One of the implications of
 136 restoring meadow hydrology is to increase plant productivity
 137 rates as well as suppress microbial respiration, leading to an
 138 increase in soil carbon storage.

139 Despite the significant attention to mountain meadow wa-
 140 tershed assessment and restoration over the past two decades,
 141 relatively few studies have investigated carbon cycling in
 142 mountain meadows directly. The FLUXNET global network
 143 of eddy flux towers has so far produced hundreds of site-years
 144 reflecting most major biomes of the world, but has produced
 145 relatively few studies of detailed carbon fluxes in mountain
 146 meadows (Oliphant 2012). The objective of this study is to
 147 investigate the carbon and water cycles of a mountain mead-
 148 ower ecosystem throughout the growing season. The meadow
 149 selected (Loney Meadow) is in the South Yuba River water-
 150 shed in the Northern Sierra Nevada, California, USA, at about
 151 1800 m elevation. Specifically, the study aims to use high-
 152 frequency, meadow-scale eddy covariance observations over
 153 a 5 month period of the growing season to (a) investigate
 154 meadow ecosystem functioning over timescales from diurnal
 155 to multi-day to seasonal, (b) assess the key environmental
 156 controls on ecosystem functioning, particularly the ability of
 157 the ecosystem to sequester atmospheric CO₂ and (c) approxi-
 158 mate the annual total meadow CO₂ exchange. The results
 159 from this study are compared to the limited results published
 160 from other meadow ecosystems as well as wetlands and grass-
 161 lands for context, and implications for the role of climate and
 162 land use changes on meadow carbon sequestration are
 163 discussed.

164

Biophysical Setting and Methods

165

Biophysical Setting

166

Loney Meadow is located on the upper western flank of the Northern Sierra Nevada in the headwaters of the South Yuba River watershed, which drains west to the Sacramento River (Fig. 1). The meadow has a surface area of approximately 138,000 m² and is located at 39.421°N, −120.655°W, with an elevation near the center of 1822 m MSL. The main Loney meadow investigated in this research is a riparian low-gradient type in the Weixelman et al. (2011) classification. We expect that its hydrology is supported by surface streamflow inputs, hillslope runoff, and geologic groundwater sources; a likely input of non-gaged snowmelt-fed streams and groundwater is suggested by an 83% increase in discharge between the inflow and outflow gauge reported in 2016 from Hutchinson et al. (2020) while the contributing catchment area is only 20% greater (5.75 km² at the outflow as compared with 4.77 km² at the inflow).

182

Loney Meadow experiences mountain Mediterranean climate conditions with warm dry summers and cold wet winters. Following a three-year period of severe drought conditions in California, the 2015–16 water year experienced closer to average levels of precipitation, snowfall and temperature. Total precipitation for the 2015–16 water year of 194 cm was recorded at the Bowman Dam monitoring station located approximately 2.4 km from Loney Meadow, which was 15% higher than the long-term average between 1896 and 2020. Snowfall (454 cm) however, was 24% lower than the long-term average and temperatures were slightly above average. Daily average temperatures at Bowman Dam range between −3 °C during the winter and 26 °C in the summer with snow typically covering the ground from October to May and peak snow depth occurring in March (WRCC 2020). In a comparison of 13 northern California montane meadows studied by Reed et al. (2020), Loney was among the wettest and most productive. In 2016, the average height of groundwater (relative to a ground surface datum) using an array of 10 piezometers in Loney Meadow during the summer recession (June–September) was +0.1 m, with a minimum of −1.83 m and a maximum of +1.47 m (Hutchinson et al. 2020; Reed et al. 2020).

205

The vegetation of Loney Meadow is dominated by mixed graminoids and forbs, consistent with hydric to mesic meadow communities elsewhere in the Sierra Nevada. Vegetation sampling conducted across Loney Meadow in 2016 identified more than 120 species (Reed et al. 2020). Five of the 10 most abundant species observed were graminoids, four sedges (*Carex utriculata* (10.1% cover), *C. senta* (6.6%), *C. spectabilis* (5.1%), *C. nebrascensis* (4.9%) and the California Brome (*Bromus carinatus* - 4.7%). Other abundant species included perennial grasses and herbs such as

Sympyotrichum spathulatum (9.8%), *Juncus balticus* (5.8%), *Potentilla gracilis* (5%), *Perideridia lemmontii* (3.3%), and *Achillea millefolium* (2.8%). Reed et al. (2020) assessed that the species observed in Loney Meadow in 2016 were approximately 20% obligate wetland species and 54% facultative wetland species. Furthermore, they reported biomass estimates obtained for 2015–16 in Loney Meadow, which averaged 150 g m^{−2} for above ground biomass and root carbon of 2.2 kg m^{−2}. These observations were made in a grid pattern across the meadow surrounding the tower location, with all corners of the grid within 120 m of the flux tower location for this study, so they provide a representative sampling of the species that the flux tower ‘observes’ (Section 2.2).

Based on regular site visits and daily images captured from a digital camera mounted at the site, the meadow ecosystem transitioned through four distinct phases over the observation period from May 17th to September 6th, 2016 (Table 1). The first period saw the emergence from melting snow cover of grasses, sedges and small forbs, with rapid growth. During the early spring season, ponding occurring on over 75% of the surface, and a significant storm event provided snow cover for several days over the emerging vegetation. By July, vegetation height and density appeared to reach a maximum, and this was followed by a long period of senescence. From early July to early August, this included a changing of vegetation color with limited decrease in height and density. By the end of August, a significant decline in plant density and height had occurred and negligible green vegetation was visible (Table 1).

Loney Meadow vegetation was grazed by a small herd of cattle between late June and September 2016. Approximately 50 cow and calf pairs were released into the meadow at the end of June and were left to graze a large area around and including Loney Meadow until the end of September. The main observable impact of cattle grazing was the reduction in above ground biomass, especially during the latter part of summer when new growth declined, and the addition of manure to the surface. Cattle density on the meadow remained fairly low, and we did not see the creation of bare patches or undue compaction, although channel scouring evident in several places was likely exacerbated by their presence.

The NDVI image of the meadow in the vicinity of the tower (Fig. 1) was captured in the peak of the growing season using a drone-mounted multispectral camera (Davis et al. 2020), illustrating the high values from the meadow vegetation (yellow to green), and the low values of rocks and water. The latter indicates both the location of meadow channels and the presence of standing water (particularly to the SW of the tower). This area contained emerging vegetation and would show high NDVI if re-imaged once the standing water subsided, as the summer progressed. The image was captured in 2017, following a wetter winter than in 2016, when the

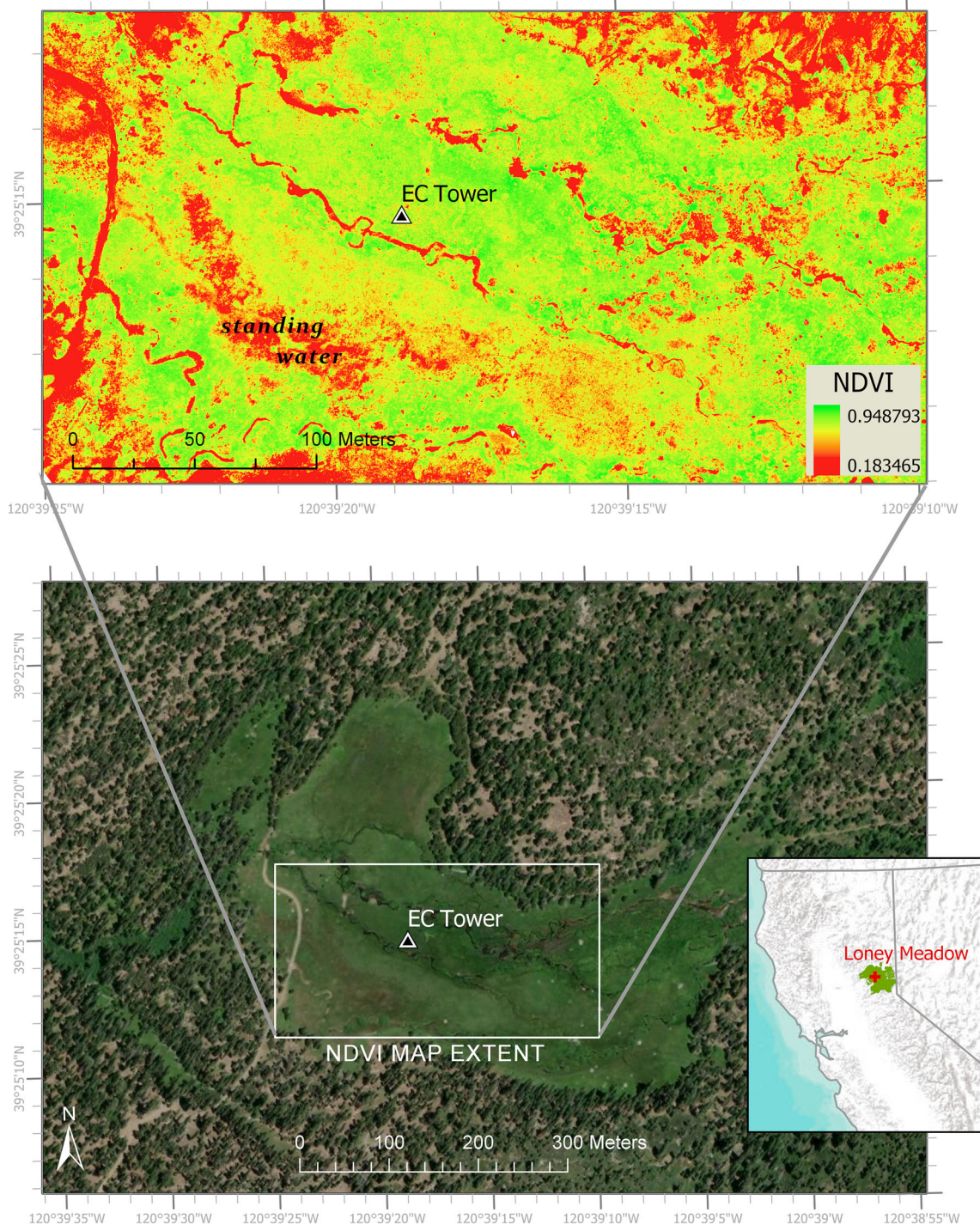


Fig. 1 Study site characteristics and eddy covariance flux measurement location including a visible image of the meadow extent (source: Esri, DigitalGlobe, GeoEye, Earthstar Geographics, CNES/Airbus DS, USDA, USGS, AeroGRID, IGN, and the GIS User Community) and a normalized difference vegetation index (NDVI = (NIR-red)/(NIR + red)) image of the meadow ecosystem within the main flux source area created from a MicaSense RedEdge radiometrically calibrated 5-band camera

268 reported measurements were made. The standing water was
269 evident in the same location in 2016, but approximately a
270 month earlier in the melt season.

mounted on a 3D Robotics Solo drone flown at 80 m above ground level with 75% overlap on July 16, 2017, processed with Pix4D Mapper to produce 5-cm pixels of reflectance in blue (20-nm band centered at 475 nm), green (20-nm band centered at 560 nm), red (10-nm band centered at 668 nm), near IR (40-nm band centered at 840 nm), and red edge (10-nm band centered at 717 nm) (Davis et al. 2020)

The soil organic matter (SOM) for Loney Meadow was found to average 234 g kg⁻¹ with a standard deviation of 59 g kg⁻¹, from 19 samples, which were collected in the 5–15 cm layer, randomly

t1.1 **Table 1** Climate and ecosystem conditions during four distinct phases of the growing season

Period Approx. dates	1. Emergence 5/17 - 6/5/2016	2. Peak growth 6/6 – 7/5/2016	3. Early senescence 7/5 – 8/7/2016	4. Late senescence 8/8 – 9/6/2016
Air Temp. Daily (°C)	Max: 16.2 Mean: 9.6 Min: 1.7	Max: 20.4 Mean: 13 Min: 3.4	Max: 23.4 Mean: 14.5 Min: 3.6	Max: 23.5 Mean: 14 Min: 3.7
Precipitation Total (mm)	34	0.5	0	0.5
Soil Moisture (m ³ m ⁻³)	0.53	0.47	0.23	0.10
Vegetation Condition	Emergent phase, surface mostly saturated	Maximum vegetation height & density	Vegetation color change, density remained high	Decline in living biomass and height
Vegetation Height (cm)	1-10 cm	30-65 cm	30-50 cm	20-30cm
Image: Noon, west-facing, from 2.2 m				

sampled from an area of about one hectare near the center of the meadow at different times during the summer of 2016. These values were obtained using the loss on ignition (LOI) technique, with soils subjected to 360 °C temperatures for 2 h, after 24 h of drying at 105 °C. Roche et al. (2014) found similar but slightly higher values for the same depths across nine ‘moderately wet’ and ‘wet’ montane meadows in the Sierra Nevada. These values are also similar to and slightly higher than those found by Maher (2015) for a restored montane meadow. Both of these previous studies also sampled dry or degraded meadows, which were universally lower in SOM than was found for Loney Meadow. Additionally, Hutchinson et al. (2020) reported values of approximately 7.4 kg m⁻² soil carbon averaged over 2016 and 2017 for Loney Meadow, and these values were similar to those found elsewhere in Northern California mountain meadows (e.g. Plumas Corporation 2020). The U.S. Forest Service (USFS) and National Fish and Wildlife Foundation (NFWF) had identified Loney Meadow as ‘degraded’ at the time of this study, and low-impact restoration work to help reduce channel discharge in several locations was conducted in the following year. This appears to have resulted in wetter habitat conditions based on results of hydrologic, soil and vegetation monitoring over the period 2015–2019 (Hutchinson et al. 2020). Nevertheless, based on the abundant hydric plant species, and significant soil carbon stocks observed at the time of this study, we expect the meadow ecosystem was acting as a net carbon sink overall.

300 Experimental Design

301 A micrometeorological observation system with eddy covariance (EC) instruments (flux tower) was deployed in the

302 meadow between May 17th and September 6th, 2016. The 303 location of the flux tower slightly to the west of center, was 304 selected in order to ensure reasonable measurement length 305 across the meadow surface during both the dominant westerly 306 up-valley winds observed during the day and down-valley 307 drainage flows from the east at night, which produce a longer 308 measurement footprint due to the stable nocturnal boundary 309 layer (Fig. 1). The eddy covariance system was comprised of a 310 3-dimensional sonic anemometer-thermometer (CSAT3, 311 Campbell Sci., Logan, Utah, USA) and an open path infrared 312 gas analyser (Li7500, LiCor Inc., Lincoln Nebraska, USA), 313 which were deployed at 2.44 m above ground level (approx- 314 imately four times the maximum canopy height). These were 315 sampled at 10 Hz by a CR3000 data logger (Campbell Sci., 316 Logan, Utah, USA). In addition, 30-min average radiation 317 fluxes were measured using a four-component radiometer 318 (NR01, Hukseflux, Delft, The Netherlands) deployed at 319 1.2 m and air temperature and relative humidity were 320 measured at 2.44 m using a HMP45C probe (Vaisala Corp., 321 Helsinki, Finland). A tipping bucket rain gauge (TR-5251 322 Texas Electronics, Dallas, Texas, USA) was mounted at 323 0.5 m. The soil heat flux was determined from the average 324 of direct measurements from a pair of heat flux plates (HF01, 325 Hukseflux, Delft, The Netherlands) installed at a depth of 326 5 cm combined with heat storage change estimated for the soil 327 layer above the plates from four spatial averaging thermocou- 328 ples inserted into this layer. Mean soil temperature was also 329 determined at 2 and 10 cm depths using CS107 probes 330 (Campbell Sci. Inc.) and average soil moisture in the 0– 331 15 cm depth range was determined using a CS616 TDR probe 332 (Campbell Sci. Inc.). In addition, a Moultrie game camera was 333

334 attached to the center pole of the tower at 2.2 m facing west
 335 and captured daily (midday) images of the meadow surface.

336 Data Processing, Rejection and Uncertainty

337 EC-derived fluxes of CO₂, water vapor and heat were calcu-
 338 lated from 30-min covariance blocks, after removal of spikes
 339 in the high frequency data. These fluxes were corrected for
 340 density fluctuations (WPL corrections) and planar-fit coordi-
 341 nate rotations (Lee et al. 2004). The distribution of the flux
 342 source area in the upwind direction was calculated for each
 343 30-min period using the analytical footprint model of Hsieh
 344 et al. (2000).

345 Eddy covariance measurements have been shown to under-
 346 estimate the flux under conditions of low turbulent energy
 347 (Massman and Lee 2002; Papale et al. 2006; Burba 2013).
 348 The friction velocity (u^*) threshold for rejection varies based
 349 on the ecosystem being sampled and typically ranges between
 350 0.05 and 0.2 m s⁻¹ (Massman and Lee 2002). Using the meth-
 351 od of Papale et al. (2006) to determine a site-specific u^*
 352 threshold, the rejection threshold for this site was established
 353 at $u^* >= 0.1 \text{ m s}^{-1}$. This criterion caused the most frequent
 354 rejection of data, with a strong bias toward nocturnal hours.
 355 Loney Meadow also provides a challenge for EC measure-
 356 ments due to its relatively small size. The meadow boundary
 357 was defined from analysis of satellite imagery (Fig. 1) and the
 358 radial distance from the tower to the meadow boundary was
 359 evaluated for 21 directions. For each 30-min flux, data were
 360 defined as acceptable if the 90th percentile of the source area
 361 distance in the upwind direction was less than the distance to
 362 the meadow boundary. This ensured accepted flux data were
 363 representative of the meadow plant communities. Over the
 364 entire study period, the 90th percentile of the flux source in
 365 the upwind direction ranged from a few meters to more than
 366 600 m, though averaged 90 m, with a standard deviation of
 367 49 m. Thus, the eddy covariance CO₂ and H₂O flux observa-
 368 tions mostly represent the same area in which plant sampling
 369 was conducted, and therefore represents biophysical processes
 370 driven by the plant community described in Section 2.1.

371 Understanding uncertainty in EC observations can be ad-
 372 ditionally challenging in complex terrain, particularly with
 373 heterogeneous vegetation and during calm conditions when
 374 local scale atmospheric circulations dominate (Castellví and
 375 Oliphant 2017). Though these are generally larger than the
 376 flux footprint scale, they potentially add a local scale signal
 377 to vertical transport that is unmeasured by EC. Since all com-
 378 ponents of the surface energy balance were directly measured
 379 (assuming heat storage changes were minimal in the short
 380 meadow vegetation), closure of the energy balance was used
 381 as an independent check on the quality of the EC measure-
 382 ments. This is normally assessed by the linear relationship
 383 between the combined EC-derived heat fluxes (sensible and
 384 latent heat flux) and available energy (difference between net

radiation and ground heat flux) on a 30-min basis (e.g. Wilson
 385 et al. 2002). In this case, the slope of the linear model for all
 386 acceptable data was 0.67 ($r^2 = 0.88$). These values did not
 387 change significantly when applied to four subsets of data
 388 representing the four different phenological stages identified
 389 in Table 1. This slope value is slightly lower than average but
 390 well within the distribution of closure estimates from synthe-
 391 sis studies comparing multiple sites (e.g. Wilson et al. 2002)
 392 and were similar to other studies in complex terrain (Stoy et al.
 393 2013), especially a similar meadow in the Sierra Nevada
 394 (Castellví and Oliphant 2017). The coefficient of determina-
 395 tion as well as the slope value suggests that the EC fluxes
 396 presented here are strongly correlated with the actual turbulent
 397 fluxes but consistently underestimate them.

398 Volumetric soil water content was measured using a Time
 399 Domain Reflectometry probe (TDR), with 30 cm probe
 400 lengths, which were inserted at a 30° angle relative to the
 401 surface, thus producing an average measurement in the layer
 402 0–15 cm. The probes were carefully inserted into firm soil
 403 ensuring good contact between the soil and probes along their
 404 entire lengths. Well-sited TDR probes provide an excellent
 405 record of soil moisture change over time, although site cali-
 406 bration is recommended to control the absolute magnitude,
 407 particularly in more porous soils and those with high organic
 408 content (Zegelin et al. 1992). Gravimetric soil water content
 409 was determined during site visits from 16 soil samples collect-
 410 ed in random locations within 100 m of the TDR probe/flux
 411 tower at a depth of 5–15 cm with a hand trowel and aluminum
 412 soil tins. To convert these to volumetric soil water content for
 413 comparison with the TDR, we used a bulk density of
 414 0.54 Mg m⁻³ based on observations by Baccei et al. (2020)
 415 and Reed et al. (2020) in numerous Sierra Nevada meadows.
 416 Resulting volumetric water content ranged from 50% during
 417 the early wet phase when standing water was observed nearby
 418 to around 10% in early September and comparison with the
 419 TDR probe for the five soil sampling periods produced a lin-
 420 ear fit with a zero offset, a slope of 0.98 and a coefficient of
 421 determination of 0.98.

423 Partitioning and Gap Filling CO₂ Exchanges

424 In carbon budget terms, the 30-min EC-derived CO₂ flux
 425 equates to the net ecosystem exchange of CO₂ (NEE , mgC
 426 m⁻² s⁻¹). NEE is the net result of two much larger and
 427 directionally opposing CO₂ exchange processes; gross prima-
 428 ry production by photosynthesis (GPP) which causes an
 429 atmosphere-to-ecosystem flux of carbon, and ecosystem res-
 430piration (R_E) which causes an ecosystem-to-atmosphere flux,

$$431 NEE = R_E - GPP \quad (1)$$

432 Eq. 1 produces the meteorological sign convention for NEE
 433 where positive values indicate a net ecosystem source of CO₂

to the atmosphere and negative values indicate a net ecosystem sink. The relative contributions of GPP and R_E to an eddy covariance measurement of NEE are not directly observed by EC. However, since these plant species require light for photosynthesis, it can be assumed $R_E \approx NEE$ (observed) during nocturnal hours when PAR is zero. Many studies have shown that soil temperature has a strong correlation with respiration, particularly in grasslands, but that the relationship varies with soil moisture as well as seasonal changes in plant phenology (Gilmanov et al. 2005; Papale et al. 2006; Reichstein et al. 2005). The relationship between nocturnal NEE values and bin averaged soil temperatures (T_s) was evaluated, and best described by a linear fit;

$$R_E = 0.014 T_s + 0.066, \quad r^2 = 0.95 \quad (2)$$

In order to account for the impact of soil moisture, which declined throughout the period as well as changes in phenology and biomass, the model was determined for four seasonal periods independently (as defined in Table 1). The slope of the model increased significantly throughout the summer from 0.01 to 0.019. Using the period-dependent models, 30-min R_E values were calculated for the entire study. These derived R_E values were used to gap-fill daylight periods and to replace data rejected using the QC criteria outlined above.

For daylight hours, observations of NEE were combined with modeled R_E , to calculate GPP by residual using Eq. 1. A commonly used empirical light use efficiency model based on a rectangular hyperbola (Eq. 3) was then fit to the observed data using PAR and accepted daylight GPP estimates at the 30-min timescale (after Xu and Baldocchi 2004; Gilmanov et al. 2007; Oliphant et al. 2011), such that

$$GPP = \frac{\alpha \times A_{max} \times PAR}{A_{max} + \alpha \times PAR} \quad (3)$$

where the coefficient α is the initial slope of the light-use efficiency (LUE) curve and A_{max} is the point of maximum carbon assimilation. Since LUE is expected to change through the growing season due to changes in leaf area density and chlorophyll concentration, independent models were generated and applied to the four distinct phases of the growing season identified in Table 1.

Results

Diurnal Patterns and Drivers of Ecosystem CO₂ Exchanges and Evapotranspiration

Based on ensemble averages over the observed growing season, Fig. 2 shows that the ecosystem was a strong and dynamic net sink of CO₂ from the atmosphere during the day, and a more consistent and weaker source of CO₂ to the atmosphere

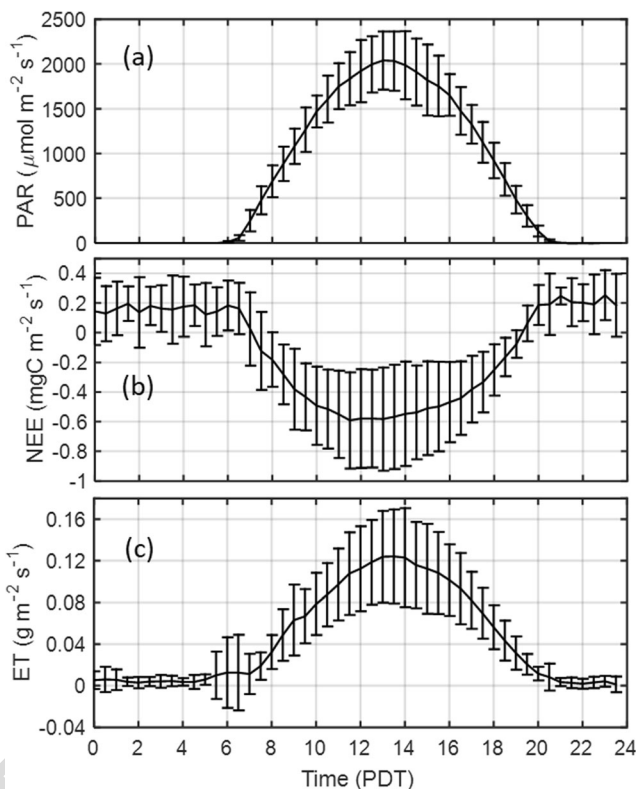


Fig. 2 Diurnal time series of 30-min ensemble averages \pm one standard deviation (error bars) of (a) PAR , (b) NEE and (c) ET observed at Loney Meadow for the entire observation period

at night. Daylight NEE values were closely anti-correlated with PAR , with an immediate response (decreasing NEE) following sunrise. The morning switch from source to sink occurred on average 45 min later, and peak sequestration rates of approximately $-0.6 \text{ mgC m}^{-2} \text{ s}^{-1}$ on average occurred by 11:30 PDT, approximately 90 min before solar noon. The net ecosystem exchange switched from a sink to a source approximately 75 min before sunset, reaching its peak soon after sunset. Though clearly driven by the symmetrical cycle of PAR , the diurnal pattern of NEE indicates a stronger response (sink) in the morning than the afternoon for the same light levels. Nocturnal NEE values remained relatively steady, declining from a little over $0.2 \text{ mgC m}^{-2} \text{ s}^{-1}$ to a little under by the end of the night (Fig. 2). The inter-diel variability of NEE is greater during the mid-day hours of peak uptake than through the night, suggesting more day-to-day control on CO₂ flux variability in photosynthesis than respiration over the growing season. The sum of the diurnal ensemble 30-min averages for the observational period was $-6.1 \text{ gC m}^{-2} \text{ d}^{-1}$, similar to mature forests in the peak of their growing season (e.g. Baldocchi 2008).

Evapotranspiration (ET) rates began to climb significantly about an hour after sunrise, with the lag closely following the switch in net radiation from negative to positive (not shown). However, ET thereafter followed a more symmetrical correlation with PAR than NEE , so the loss of water relative to carbon

uptake was less during the morning than afternoon hours. The relatively lower ET in the morning is probably related to greater atmospheric demand for water in the warmer and drier afternoon hours relative to the morning hours for the same levels of PAR . There was also a secondary small peak in mean ET around sunrise as well as a much larger inter-diel variability. Assessment of the raw data reveal that this resulted from small spikes on some mornings at this time, suggesting evaporation of dewfall, which was also visually observed occasionally during site visits. Although close to zero at night on average, the standard deviation bars for ET descending below zero suggests that water deposition on the leaves occurred on some nights.

Decomposition of the diurnal cycle into partitioned CO_2 fluxes, as well as key environmental drivers for four different seasonal periods are shown in Fig. 3, with daily magnitudes provided in Tables 1 and 2. The diurnal pattern of NEE was clearly driven most strongly by GPP , which was closely correlated with PAR . The diurnal pattern of GPP remained mostly symmetrical in each of the four seasonal periods, though at very different magnitudes throughout the growing season. Relative to the pattern of PAR , there is a flattening during the mid-day hours, suggesting a lower light use efficiency during those hours. In the senescent period, this flattening occurred from about 1100 to 1700 PDT and peaked at only $0.5 \text{ mgC m}^{-2} \text{ s}^{-1}$, compared with a diurnal peak of $1.26 \text{ mgC m}^{-2} \text{ s}^{-1}$ during the period of strongest growth (Period 2). Differences within the growing season can be less easily explained by PAR . The emergent phase had the 2nd highest GPP but the lowest PAR , and the senescence onset period (Period 3) had the highest available PAR but produced a 33% decline in diurnal peak GPP . This shift coincided with a significant reduction in volumetric water content (VWC), and an increase in vapor pressure deficit (VPD).

R_E followed the somewhat asymmetrical diurnal cycle governed by soil temperature but also showed distinct seasonal differences (Fig. 3c). The diurnal range in R_E is only about one quarter of the range in GPP . On a seasonal basis, the emergent phase exhibited the lowest R_E rates. This was also the period with the lowest soil temperature (Fig. 4e) and highest soil water content (Fig. 4f). The high water table during this period (water flowed across majority of the meadow) would likely suppress root and soil respiration as with other

wetlands (e.g. Knox et al. 2015). The three following seasonal periods had similar daily average R_E rates to each other, and about 20% higher than the wet emergent phase (Table 2). However, the peak value of R_E consistently increased as the season progressed, reaching a maximum of about $0.38 \text{ mgC m}^{-2} \text{ s}^{-1}$ during the senescent phase (Fig. 3b).

Seasonal and Weather Controls on Ecosystem CO_2 Exchange

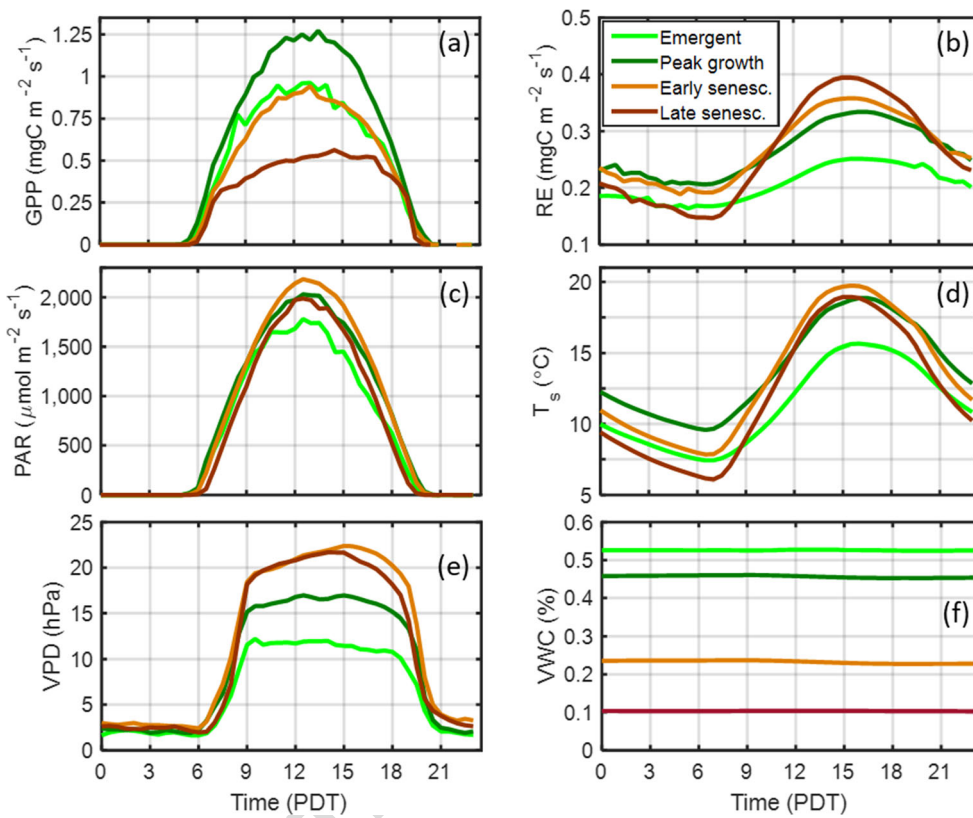
Daily total NEE fluctuated significantly both at seasonal and synoptic scales, but resulted in a net sink of CO_2 on 82 of the 112 days measured (Fig. 4). The emergent period until May 19th (DOY 160) produced a decline in NEE (increasing sink of CO_2) as leaf area index (LAI) rapidly increased, punctuated by sharp increases in NEE in response to a significant early summer storm. The impact of the storm resulted in the ecosystem switching from a net sink to source of CO_2 on two of the days. During the storm, PAR decreased significantly (88%) due to deep cloud cover, which coincided with a similarly large decline in GPP (80%). Daily average air temperature dropped 12°C and soil temperature dropped 8°C , which coincided with a 42% decline in R_E (Fig. 4). Since the meadow was nearly saturated at this time, the main hydrologic impact on NEE was the partial coverage of the meadow with snow, which would have shielded emerging vegetation from PAR and helped suppress soil and plant respiration. From Day 160 (May 19th) to Day 187 (July 5th) NEE reached its peak uptake and remained fairly constant, with weather disturbances having a smaller impact. Throughout this period PAR remained high, volumetric soil water content was above 40% and very high daily totals of carbon sequestration occurred (-20 and $-25 \text{ gC m}^{-2} \text{ d}^{-1}$). This period was also characterized by maximum vegetation height and density (Table 1).

From Day 187 (July 5th) a steady rise in NEE began, which continued to the end of the study, and resulted in the meadow ecosystem switching from a net sink to a source on a daily basis around Day 224 (August 11). Despite maintaining high values for PAR , this rise in NEE coincided with decreasing volumetric soil water content from 40% to 10%, and appeared to be directed by changes in GPP , which declined steadily throughout this period. Senescence is also evident in shift in vegetation color from daily surface images (Fig. 4).

t2.1 **Table 2** Daily total CO_2 fluxes calculated for each seasonal period by the sum of the 30-min ensemble averages for each period, Loney Meadow, 2016 growing season

	Emergence (May 17 – Jun 5)	Peak growth (Jun 6 – Jul 5)	Early senescence (Jul 6 – Aug 7)	Late senescence (Aug 8 – Sep 6)
t2.3 $GPP (\text{gC m}^{-2} \text{ d}^{-1})$	34.05	42.96	31.06	18.78
t2.4 $R_E (\text{gC m}^{-2} \text{ d}^{-1})$	17.42	21.6	22.51	20.32
t2.5 $NEE (\text{gC m}^{-2} \text{ d}^{-1})$	-13.65	-18.51	-5.48	2.97

Fig. 3 Diurnal ensemble 30-min averages of GPP (a), RE (b), PAR (c), soil temperature (T_s) (d), vapor pressure deficit (VPD) (e), and volumetric water content (VWC) (f) according to seasonal period, Loney Meadow, 2016



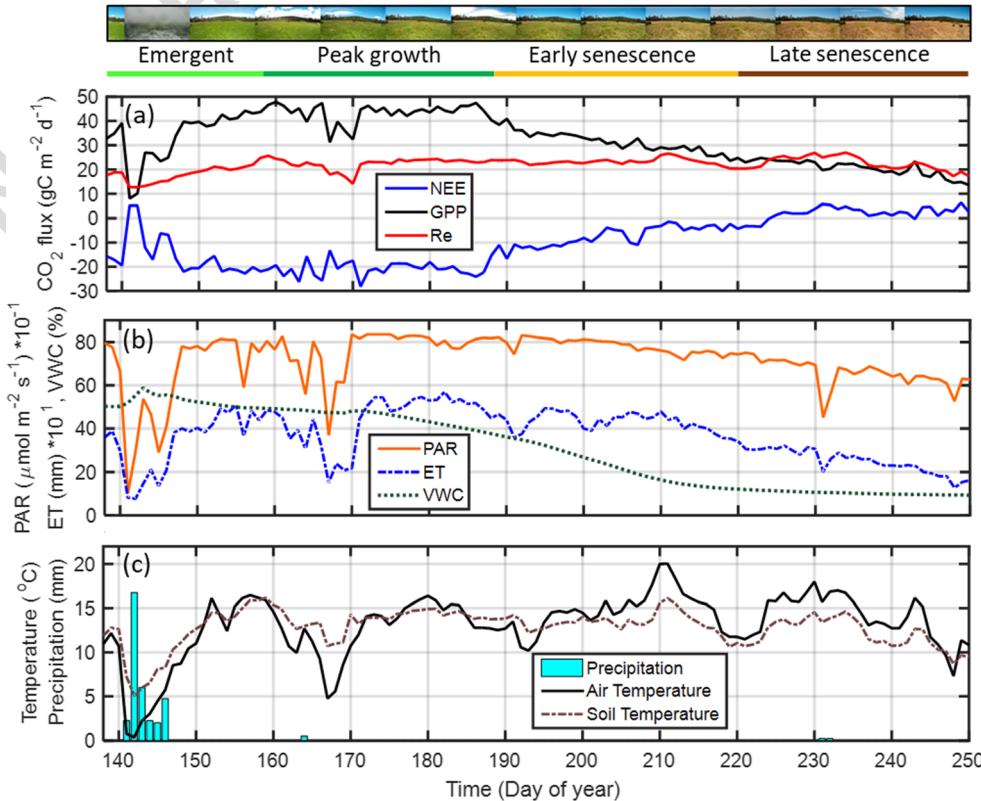
593
594

Respiration by comparison remained fairly constant throughout this period. A small rain event (< 1 mm) occurred on

August 18 (Day 231), but had little to no impact on recorded soil moisture levels (Fig. 4c & d). At this point, most of the

595
596

Fig. 4 Daily total ecosystem CO_2 and H_2O exchanges and environmental conditions at Loney Meadow during the 2016 growing season. At top is time sequence of approximately weekly images of meadow surface taken from 2.2 m a.g.l., west facing at noon, and illustration of the four seasonal periods distinguished



597 vegetation had become insensitive to light levels and productivity was constrained by water availability. Throughout the
 598 growing season, ET more closely followed GPP than soil moisture, suggesting the dominance of transpiration.
 599 However, during cloudy periods, as indicated by PAR in
 600 Fig. 4b, ET declined more significantly than GPP , raising
 601 the water-use efficiency on those days.
 602

603 In comparison to other meadow ecosystems surveyed using
 604 the EC method, the daily CO_2 flux magnitudes found in
 605 Loney Meadow (averaging $-18.51 \text{ gC m}^{-2} \text{ d}^{-1}$) were signifi-
 606 cantly higher (larger negative value). A seasonal peak daily
 607 total CO_2 flux of $-3.9 \text{ gC m}^{-2} \text{ d}^{-1}$ was observed in an alpine
 608 meadow on the Tibetan Plateau (Kato et al. 2004), -6.3 gC
 609 $\text{m}^{-2} \text{ d}^{-1}$ for a meadow steppe ecosystem in Northeast China
 610 (Dong et al. 2011) and $-7 \text{ gC m}^{-2} \text{ d}^{-1}$ for a montane meadow
 611 at 1450 m MSL in the Sierra Nevada, California following a
 612 very dry winter (Maher 2015). Loney Meadow was also
 613 among the most productive ecosystems in comparison to
 614 grasslands and wetlands observed elsewhere. For example,
 615 the highest recorded daily CO_2 exchange in a young wetland
 616 studied by Knox et al. (2015) was about $-11 \text{ gC m}^{-2} \text{ d}^{-1}$ and a
 617 survey of wetlands by Lund et al. (2010) showed maximum
 618 daily total NEE values ranging between -1 and -4 gC m^{-2}
 619 d^{-1} . Grasslands exhibit a high degree of variability in peak
 620 daily total CO_2 values ranging between -5 (Flanagan et al.
 621 2002; Xu and Baldocchi 2004) and $-50 \text{ gC m}^{-2} \text{ d}^{-1}$ (Dugas
 622 et al. 1999). The latter noted that daily fluxes lower than -20
 623 $\text{gC m}^{-2} \text{ d}^{-1}$ are typically rare and generally short-lived.
 624

625 Light, Carbon and Water Relationships in the Meadow 626 Ecosystem

627 The coefficients and statistics of rectangular hyperbola LUE
 628 curve fitting are provided in Table 3. Both the initial slope of
 629 the curve (α value) and the point of maximum CO_2 assimilation
 630 (A_{max}) are high compared to grasslands, especially during the
 631 emergent and peak growth phases. In a comparison, LUE of
 632 twenty European grasslands, Gilmanov et al. (2007) reported α
 633 values ranging from 0.016 to 0.075 and A_{max} values ranging from
 634 42.5 to 216 $\mu\text{mol m}^{-2} \text{ s}^{-1}$, with the higher values attributed to
 635 wetter grasslands. The light response parameters observed in

636 Loney Meadow for the full observation period was close to the
 637 maximum of these grassland sites and exceeded them all during
 638 the peak growth phase. The beginning of senescence produced a
 639 decline in both the magnitude and consistency in LUE and the
 640 late senescence showed heavily suppressed photosynthesis and a
 641 largely disconnected relationship with PAR .
 642

643 The relationships between GPP and both PAR and ET at
 644 the daily timescale are presented in Fig. 5. Although the mag-
 645 nitude of GPP was generally much higher during the emer-
 646 gent and peak growth phases than the senescent phases (by
 647 12–18 $\text{gC m}^{-2} \text{ d}^{-1}$), the slope of the relationships remained
 648 fairly similar. This suggests the ecosystem maintained fairly
 649 consistent light use and water use efficiencies throughout the
 650 growing season, despite operating at very different levels of
 651 productivity. By comparison with similarly defined values for
 652 WUE reported elsewhere, the fairly consistent value of about
 653 5.5 g kg^{-1} found for Loney Meadow is quite high. In a sum-
 654 mary of WUE from 43 different ecosystems, similar values
 655 were found for deciduous broadleaf and mixed forests, but
 656 grasslands were on average significantly lower (Beer et al.
 657 2009). In this comparison, Loney Meadow would be ranked
 658 2nd of 43. However, a steppe meadow ecosystem in Northeast
 659 China produced similar mean WUE values (Dong et al. 2011),
 660 with highest WUE occurring during the peak of the warm wet
 661 growing season. This site also produced evidence of a
 662 drought-induced lowering of WUE . Ponton et al. (2006) sim-
 663ilarly found a negative correlation between daily WUE and
 664 maximum daily vapor pressure deficit for both forests and
 665 grasslands. In the current study, since soil moisture was driven
 666 by runoff more than precipitation during the summer months,
 667 the largest inter-diel differences in either LUE or WUE were
 668 caused by cloudiness. Cloudy days reduced PAR , GPP and
 669 ET , but increased both LUE and WUE . The former is likely to
 670 be due to the higher use efficiency of scattered light than direct
 671 beam, and the latter due to the lower vapor pressure deficit
 672 found on those days.

Estimate of 2016 Annual NEE at Loney Meadow

673 A direct estimate of the annual total net ecosystem exchange
 674 of CO_2 was not possible because observations did not span the

Q2 t3.1 **Table 3** Light response curve parameters (Eq. 4) and fit statistics using 30-min averages with average observed GPP

t3.2	Seasonal Period	α	A_{max} ($\mu\text{mol m}^{-2} \text{ s}^{-1}$)	r^2	n	Average GPP ($\text{gC m}^{-2} \text{ d}^{-1}$)
t3.3	All observations	0.0741	154.3	0.41	2548	32.30
t3.4	Emergent	0.0849	173.7	0.57	411	34.05
t3.5	Peak Growth	0.0861	246.7	0.82	718	42.96
t3.6	Early Senesc.	0.0609	172.9	0.67	766	31.06
t3.7	Late Senesc.	0.223	47	0.08	637	18.78

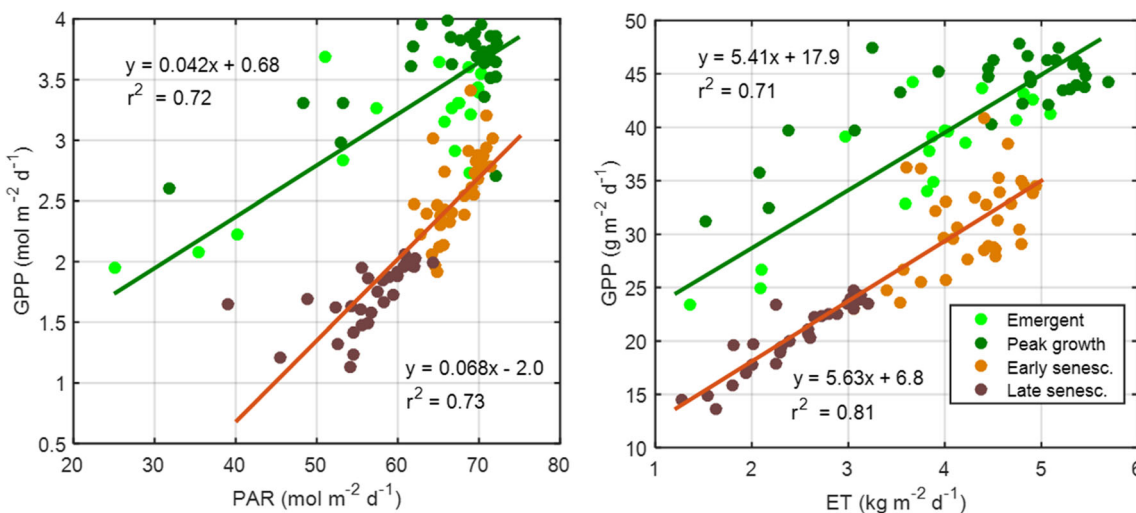


Fig. 5 Relationships between daily total *GPP* and (a) *PAR* and (b) *ET* for different seasonal periods. Linear models and coefficient of determination correspond with adjacent lines, which are derived from a combination of the two sub-periods

complete annual cycle. However, since most of the growing season was captured by the eddy covariance record and the meadow is covered by snow for about 5 months of the year, an approximation is possible, with some reasonable assumptions. First, we assumed ecosystem photosynthesis began around April 25th 2016, when it was observed that approximately 75% of the meadow surface was still covered by snow but that it was melting quickly and new shoots were beginning to emerge across the meadow. The second assumption was that the rates of change in daily *GPP*, *R_E* and *NEE* trended similarly at the beginning of the emergent phase as during the latter portion that was observed. The rates of change in observed daily *GPP*, *R_E* and *NEE* during the growing season were found to follow a linear trend, which was extrapolated backward from the beginning of observations (May 17th) to the beginning of the snow-free phase (April 25th) to estimate daily totals for each day in between. Daily values from the final senescent phase were similarly extrapolated forward from the end of the observational record to the beginning of snow cover, which was determined to be November 24th 2016, using snow depth data from a nearby climate station (SNOWTEL: Robinson Cow Camp, Elevation: 1975 m MSL). The final assumption was that ecosystem photosynthesis was zero but that soil respiration continued beneath the snowpack. It has been found that respiration from organic soils through winter snowpacks tends to be small but not negligible. This is because microbial activity can be significant in organic soils in near and even below freezing conditions but that the snowpack limits oxygen supply to the soil, increasing concentrations of CO₂ in the snowpack (Sommerfeld et al. 1993). Previous estimates of soil respiration beneath snowpacks include approximately 0.52 gC m⁻² d⁻¹ found both for a wet meadow (Knowles et al. 2016) and a deciduous forest floor (Hirano 2005), 1 gC m⁻² d⁻¹, for mountain grasslands in Switzerland (Wohlfahrt et al. 2008), and 0.7 to 2 gC m⁻² d⁻¹ for alpine and subalpine meadows respectively (Sommerfeld et al. 1993). Given the

organic soils and large growing season productivity at Loney Meadow, here we made the assumption that Loney meadow winter respiration rates beneath a snowpack was at the higher end of this range (~2 gC m⁻² d⁻¹). Daily *NEE* totals were calculated for the observation period using the high quality observations of *NEE* and gap-filled data when observational data did not pass quality control tests. We then combined these with the extrapolated values found for the unmeasured beginning and end of the snow-free period, and the estimated values from the literature for the period with snowpack to produce an annual record. This resulted in an estimated annual carbon sink of ~313 gC m⁻² a⁻¹. Hirano (2005) showed that CO₂ efflux more than doubled in the approximately 2 week period following snowmelt, due to both built-up CO₂ in the snow and soil air parcels that is released, and invigorated microbial respiration. If we factor a two-fold increase in CO₂ efflux for 2 weeks following snowmelt, the annual sink reduces to ~285 gC m⁻² a⁻¹. It is also possible that soil respiration under the snowpack followed a more modest level previously observed (~1 gC m⁻² a⁻¹), in which case the annual sink would be as high as ~450 gC m⁻² a⁻¹. These annual estimates are fairly crude but suggest Loney Meadow is a significant sink of carbon on an annual basis. Reed et al. (2020) used soil carbon and biomass measurements to estimate net soil carbon fluxes from 13 montane meadows of the Sierra Nevada and found Loney Meadow to be the largest sink at 847.7 gC m⁻² y⁻¹.

Despite having a similar seasonal pattern of *NEE* and potentially reaching large daily magnitudes of CO₂ uptake during the peak of the growing season, most grasslands observed in related climates sequester significantly less CO₂ from the atmosphere annually than Loney Meadow appears to. Annual values tend to range from ~50 to ~160 gC m⁻² a⁻¹ during years with sufficient precipitation (e.g., Ma et al. 2007; Dong et al. 2011) to annual sources from 50 to 100 gC m⁻² y⁻¹ under drier conditions (Flanagan et al. 2002; Ma et al. 2007; Scott et al. 2010). Water availability and its timing is

745 consistently identified as a driving environmental control on
 746 annual *NEE* of grasslands and several studies show this can
 747 cause a switch from a net carbon sink to source between years
 748 (Flanagan et al. 2002; Wohlfahrt et al. 2008; Scott et al. 2010;
 749 Dong et al. 2011). A synthesis study of wetland ecosystems
 750 consisting of peatlands and tundra by Lund et al. (2010) re-
 751 ported average annual net CO₂ uptake of -103 ± 103 gC m⁻²
 752 a⁻¹. The two most similar sites, with annual carbon sinks of
 753 about -200 gC m⁻² a⁻¹, were fen type wetlands with high
 754 vegetation density. Not far from Loney Meadow but near
 755 sea level, Knox et al. (2015) observed an annual *NEE* of
 756 -397 gC m⁻² a⁻¹ in a dense mature wetland in the
 757 Sacramento/San Joaquin Delta of California. Loney
 758 Meadow is likely to be a significantly larger sink than the
 759 global average of -156 gC m⁻² a⁻¹ based on 1459 site-years
 760 of data collected from flux towers covering terrestrial ecosys-
 761 tems around the planet (Balodochi 2014).

762 Discussion

763 Implications for the Carbon Cycle in Mountain 764 Meadows

765 The results from this study indicate that mountain meadows
 766 such as Loney Meadow can be large sinks for atmospheric
 767 CO₂, with highly dynamic seasonal variability. This appears
 768 to be mostly due to the unique hydrology of mountain meadows
 769 which can provide moisture to the root zone of meadow eco-
 770 systems during summer despite a lack of precipitation, produc-
 771 ing a unique seasonal signal for the eco-climate region.
 772 Furthermore, meadow soils have been found to be high in or-
 773 ganic content to significant depths, suggesting net annual car-
 774 bon uptake and longer term storage of carbon in the substrate.
 775 Snow cover in winter and water saturation in spring likely helps
 776 limits the loss of organic matter by heterotrophic respiration.
 777 There may be some loss of dissolved carbon from the meadow
 778 via the stream network, and additional losses of carbon to the
 779 atmosphere in the form of methane emissions produced during
 780 saturated soil conditions, and also emitted from grazing cattle.
 781 A fuller discussion of the likely role of cattle on the meadow
 782 carbon cycle is discussed in the following section.

783 The Loney Meadow ecosystem sequestered CO₂ at rates
 784 similar to mature wetlands and productive forests. The net
 785 CO₂ flux observed in this study was more than double that
 786 measured during an above average precipitation year in a
 787 California grassland. Yearly precipitation totals that impacted
 788 this study were close to (slightly higher) than average and
 789 followed a multi-year severe drought. Despite this, the mead-
 790 low produced abundant vegetation and acted as a significant
 791 sink over the annual cycle. This was also found by Reed et al.
 792 (2020) using assessment of carbon stocks in soil and vegeta-
 793 tion. They found Loney to be the largest annual sink of 13 SN

794 meadows, although their estimate of more than 800 gC m⁻²
 795 a⁻¹ is 2–3 times higher than the estimate we produced using
 796 eddy covariance. Their value is also extremely high in com-
 797 parison to annual estimates of a wide range of global ecosys-
 798 tems (e.g. Baldocchi 2014). The two methods for estimating
 799 the annual carbon flux are very different, and have different
 800 assumptions and weaknesses. For example, eddy covariance
 801 has a tendency to under-estimate the total flux, though this
 802 error is typically about 10–20% (e.g. Stoy et al. 2013). In
 803 addition, we were only able to measure over the growing
 804 season, and had to make many assumptions about winter
 805 and early spring fluxes. The soils approach, on the other hand,
 806 has coarse temporal coverage, which can describe only gen-
 807 eral seasonal changes in CO₂ exchanges, but not the impacts
 808 of meteorology on day-to-day variability or diurnal variability
 809 in soil temperature and plant functioning. We find significant
 810 variability in CO₂ fluxes over these timescales. On the other
 811 hand, the spatial sampling should be similarly representative
 812 of the meadow ecosystem for both techniques. This disparity
 813 in the annual carbon budget points to the need for further
 814 comparisons between carbon fluxes obtained from the two
 815 different techniques for a range of meadows. In addition, the
 816 information provided by the two techniques is highly comple-
 817 mentary and could be combined. The eddy covariance method
 818 provides a direct measure of the CO₂ exchange rate with ex-
 819 cellent temporal resolution but cannot directly ascertain the
 820 individual components and drivers of the gas flux, which is
 821 a strength of the approach of Reed et al. (2020).

822 Though the number of site years of mountain meadow
 823 observations are few, the comparison between this and other
 824 studies in China, Europe and elsewhere in the Sierra Nevada
 825 suggests mountain meadow ecosystems are highly complex
 826 and show a great deal of variability compared to other ecosys-
 827 tems. Factors that may contribute to this variability are eleva-
 828 tion, latitude, watershed characteristics, precipitation, tempera-
 829 ture and meadow hydrogeomorphology. The results present-
 830 ed here agree with other studies that show soil moisture levels
 831 in the root zone appear to be the main environmental driver
 832 (along with temperature) that controls the larger seasonal
 833 trends as they relate to plant functioning and the resulting
 834 carbon cycling. This means that mountain meadows have
 835 great potential to help sequester atmospheric carbon, but that
 836 their capacity to provide this role is highly dependent on soil
 837 moisture levels throughout the growing season, making them
 838 susceptible to changes in both climate and land use.

839 Implications for Meadow Carbon Cycling of Land-Use 840 and Climate Change

841 This study and previous research conducted in SN meadows
 842 have indicated that water availability shows a strong positive
 843 relationship to ecosystem productivity. Channel incision,
 844 resulting from degradation, effectively lowers the water table

845 and reduces water available in the root zone. Any decrease in
 846 soil moisture availability in the meadow due to water table
 847 lowering will likely reduce net ecosystem uptake of CO₂,
 848 and potentially cause a switch from a sink to a source of
 849 CO₂. On a seasonal basis, this switch occurred when volumet-
 850 ric soil moisture content dropped below about 12%.
 851 Temperature and PAR are also likely to play a role in the
 852 senescent phase although, in this case, temperatures and solar
 853 radiation remained seasonally high while both soil moisture
 854 and vegetation productivity declined. If restoration of degrad-
 855 ed meadows to raise the water is successfully implemented,
 856 there is potential to increase carbon uptake and to retain higher
 857 levels of photosynthesis later in the growing season.

858 Above-ground biomass consumption, animal respiration,
 859 digestive release of methane, soil compaction, and excretion
 860 deposits are all likely impacts from grazing cattle on meadow
 861 carbon cycles (Jerome et al. 2014; Roche et al. 2014). Cattle
 862 grazing in Loney Meadow during the study period was low
 863 density, yet the wet meadow vegetation clearly provided ex-
 864 cellent forage and evidence of reduced biomass from grazing
 865 and feces deposition was widespread. Sousanna et al.
 866 (Soussana et al. 2007) found that 25–40% of cattle forage
 867 intake is returned to the soil as non-digestible carbon (e.g.
 868 feces), while a larger portion is removed from the ecosystem
 869 as live weight (LW) gained during grazing. Some of the net
 870 carbon sink we have recorded for Loney Meadow was there-
 871 fore lost from the meadow as LW gain. Tofastrud et al. (2020)
 872 found the weight gain of a range of early maturing beef cows
 873 grazing at low stocking density averaged 24 kgC per growing
 874 season. If we use this value and assume all of the weight gain
 875 was obtained from Loney Meadow vegetation, the carbon loss
 876 from the meadow by cattle weight gain for the Lonwy 2016
 877 grazing season would be 17 gC m⁻², which represents a small
 878 but significant reduction of our estimated net carbon sink.

879 The cattle also directly impact the meadow carbon budget
 880 through autotrophic respiration of CO₂ and the digestive re-
 881 lease of CH₄. Some of the respiration of CO₂ from grazing
 882 cattle would have been recorded by the instruments when
 883 cows were grazing in the meadow upwind of the flux tower.
 884 We can approximate the magnitude of the annual flux inde-
 885 pendently based on the number of animals, number of days on
 886 site and using the daily estimate of cattle CO₂ emissions of 2.6
 887 kgC d⁻¹ per livestock unit (Jerome et al. 2014). If we assume
 888 the cattle only grazed Loney, we get an upper estimate of
 889 cattle respiration of approximately 150 gC m⁻² a⁻¹, which is
 890 small compared to the estimated annual meadow respiration
 891 of over 4 kg m⁻² a⁻¹. Some portion of this would be contained
 892 in the estimate provided by the eddy covariance measure-
 893 ments, although this portion is impossible to estimate due to
 894 the low grazing density and lack of positional data for the
 895 cattle. From both visual observations during site visits and
 896 images captured by the wildlife camera, it is clear that cattle
 897 respiration would be recorded by the instruments, at least part

898 of the time. We did not measure the flux of CH₄, though
 899 Sousanna et al. (Soussana et al. 2007) estimated that non-
 900 lactating cattle release between 0.33 and 0.45 gCH₄ kg⁻¹
 901 living weight per year. If we assume the larger of these values,
 902 and multiply by the total stock estimated living weight, and
 903 again assume that cattle only consumed Loney Meadow veg-
 904 etation, we estimate this to be about 78 mgCH₄ m⁻². In mead-
 905 ow carbon budget terms this is very small, although it repre-
 906 sents a more significant impact to atmospheric greenhouse
 907 gasses due to the relatively high radiative forcing of CH₄.
 908 Although CH₄ fluxes were not observed in this study, Reed
 909 et al. (2018) observed a diurnally-consistent soil-atmosphere
 910 CH₄ flux of −0.65 nmol m⁻² s⁻¹ for Loney Meadow soils on a
 911 single day in the 2015 growing season. This equates to an
 912 uptake of nearly 1 mgCH₄ m⁻² d⁻¹, which is opposite in sign
 913 but similar magnitude to the estimated total cattle emissions
 914 on a daily basis.

915 These estimates of the impact of cattle on the meadow
 916 carbon budget are approximations only and the impact of live-
 917 stock on the carbon cycle has shown significant variability
 918 among cattle species, type of ingested forage, climate condi-
 919 tions, ecosystem health and management intensity (Soussana
 920 et al. 2007; Jerome et al. 2014; Roche et al. 2014).
 921 Nevertheless, these estimated direct impacts of cattle reflect
 922 a loss of carbon from the meadow, some of which was un-
 923 measured, though the overall contribution is expected to be
 924 small compared to the observed vegetation CO₂ exchanges.
 925 Further, the estimates of unmeasured components of meadow
 926 carbon fluxes suggest that our estimates of annual NEE are
 927 overestimated due to the unmeasured loss of carbon by cattle,
 928 although even a conservative accounting leaves the conclu-
 929 sion that the meadow is a strong net annual sink.

930 Depending on management intensity (e.g. stocking rate)
 931 and history, grazing can also alter plant community composi-
 932 tion, soil characteristics, and the hydrologic regime (Soussana
 933 et al. 2007; Roche et al. 2014). Drought conditions reduce
 934 GPP, making the ecosystem more vulnerable to stress caused
 935 by grazing animals, while wet, healthy meadows exhibit
 936 greater resilience to disturbance (Roche et al. 2014). Many
 937 of these impacts are long-lasting, and meadow ecosystems
 938 have been found to be particularly vulnerable to any manage-
 939 ment impacts that cause a lowering of the water table.
 940 Considering the low stocking rate and large area available to
 941 graze, the presence of livestock during the study period likely
 942 had a small direct impact of lowering the net annual carbon
 943 sequestration. It is also likely that legacy impacts from activi-
 944 ties such as grazing has degraded the natural hydrologic re-
 945 gime, creating secondary impacts on plant communities and
 946 their ability to sequester carbon. Given the relatively low plant
 947 productivity and soil carbon of degraded meadows with de-
 948 pleted water availability to plant roots, these indirect impacts
 949 on the carbon budget may be larger and are certainly longer
 950 lasting.

Similar to the effects of degradation, climate change has the potential to impact the net CO₂ potential of SN mountain meadows by altering precipitation and seasonal hydrologic inputs. Research suggests that a warming climate will reduce the amount of precipitation that falls as snow and initiate snowmelt earlier in the season, which will contribute to a longer and drier growing season (Lowry et al. 2011). Using this study as an example, climate trends suggest that the peak growth period would shorten and start earlier and the senescence period would lengthen. Since the peak growth period accounts for nearly half of the entire net CO₂ uptake measured in the 2016 growing season, a shorter peak growth period would have a significant negative impact on the overall strength of the sink on an annual basis. Similarly, a longer period of carbon release, stemming from earlier seasonal drying, will contribute to declines in annual carbon uptake. With a possible switch to a net annual loss of carbon, meadow soils would likely lose carbon to the atmosphere from stocks built up over time. Indeed, Roche et al. (2014) and Maher (2015) both found organic content in dry or degraded meadows to be significantly less than that of wet or restored meadows in the Sierra Nevada. Another potential effect of a warmer climate is increasing soil temperatures, which would likely stimulate higher respiration rates throughout the season. Furthermore, if a high water table is maintained through protection and restoration practices, it is likely that SN meadows will be more resilient to the effects of climate change and maintain their effectiveness at sequestering carbon from the atmosphere.

Conclusions

This study employed eddy covariance to investigate surface-atmosphere exchanges of CO₂ in a mountain meadow in the northern Sierra Nevada from May to September 2016. Loney Meadow acted as a strong net sink of CO₂ from the atmosphere over most of the growing season, averaging $-7.71 \text{ gC m}^{-2} \text{ d}^{-1}$. Though clearly driven by PAR, the diurnal pattern of NEE showed a slightly stronger response (sink) in the morning than the afternoon for the same light levels. At night, ecosystem respiration produced a weak but consistent source of CO₂ to the atmosphere and these rates ($\sim 0.1 < \text{NEE} < 0.3 \text{ mgC m}^{-2} \text{ s}^{-1}$) were similar throughout the measurement period.

Following snowmelt in early May, GPP increased rapidly and NEE declined so that the ecosystem became a strong sink of atmospheric CO₂, peaking at $-18.5 \text{ gC m}^{-2} \text{ d}^{-1}$. With daily total values ranging between about 10 and 50 gC m⁻² d⁻¹, GPP drove the variability in NEE throughout the growing season. GPP was governed principally by light at the diurnal and synoptic timescales and by soil water availability over the seasonal timescale. R_E rates were much smaller and more

consistent throughout the growing season than GPP, though were weakly positively correlated with temperature changes. Decline in soil moisture appeared to be the strongest control on the seasonal growth cycle and by August the ecosystem had switched from a net sink to source of CO₂ peaking at $3 \text{ gC m}^{-2} \text{ d}^{-1}$. Although the complete annual cycle was not observed, approximations of the annual budget ranged from -285 to $-450 \text{ gC m}^{-2} \text{ a}^{-1}$ depending on assumptions made. These values are closer to mature wetlands and forests, and represent a significantly higher carbon sink than most grasslands.

Using a rectangular hyperbola LUE model, the initial slope of the curve (α value) and the point of maximum CO₂ assimilation (A_{max}) were high (0.86 and 246 respectively) compared to grasslands, though the relationship weakened considerably during senescence. WUE values for Loney Meadow ($\sim 5.5 \text{ g kg}^{-1}$) were consistent and high compared with those determined equivalently from the eddy covariance record for other ecosystems. Similar to LUE, these values were closer to those found for mature wetlands and forests than grasslands. On a day-to-day basis, both LUE and WUE increased on cloudy days. This likely reflects both the higher use-efficiency of scattered light than direct beam, and the lower vapor pressure deficit experienced by the ecosystem on those days.

More long-term monitoring of the carbon exchange in SN meadows is needed to explore differences in space and time. Networks and collaborations are required to compare meadows of differing elevations, topography, level of degradation or restoration, and hydroclimate regimes. Long-term studies are required to understand inter-annual variability of carbon exchanges due to differences in snow and rainfall amounts and timing and future research should also include CH₄ fluxes since they become saturated during the spring melt. Additional measurements using chamber approaches would be helpful for deciphering the role of different plant communities within and between meadows. These approaches, along with better collaboration with the soil science community, will help provide a more complete understanding of carbon dynamics in mountain meadows. This is required to inform policymakers, land managers, and stakeholders of the likely impact of both future climates and land-use management decisions.

Acknowledgements The authors would like to acknowledge the US Forest Service for access to the meadow and South Yuba River Citizens League for field support and coordination. In particular we are grateful to Rachel Hutchinson for providing useful additional data and advice on this manuscript. The authors would also like to thank Quentin Clark for invaluable field support, the SFSU Department of Geography & Environment for providing transportation to the field site and some field sampling equipment, and the SFSU College of Science & Engineering for funds to acquire the multispectral camera and drone platform. This research did not receive any specific grant from funding agencies in the public, commercial, or not-for-profit sectors.

- 1055 **Code Availability** Not applicable.
- 1056
- 1057 **Authors' Contributions** Study conception, design and most fieldwork
1058 was conducted by DB and AO. JD conducted field collection and analysis
1059 of drone imagery. Data analysis was principally conducted by DB and
1060 AO and the initial manuscript was drafted by DB. All authors worked on
1061 all drafts of the manuscript thereafter, with particular focus on meadow
1062 hydrogeomorphology by JD and biometeorological aspects by DB and
1063 AO. All authors read and approved the final manuscript.
- 1064 **Funding** External funding was not available for this study.
1065 Transportation for fieldwork was provided by San Francisco State
1066 University, Dept. of Geography & Environment.
- Q3 1067 **Data Availability** All data used in this study are freely available by
1068 contacting the corresponding author.
- 1069 **Declarations**
- 1070 **Ethics Approval** Not applicable.
- 1071 **Consent to Participate** Not applicable.
- 1072 **Consent for Publication** Not applicable.
- 1073 **Conflicts of Interest/Competing Interests** The authors have no conflicts
1074 of interest or competing interests related to material in this study.
- 1075 **References**
- 1076 Allen BH (1987) Forest and meadow ecosystems in California.
1077 *Rangelands* 9:125–128 <http://www.jstor.org/stable/3901046>
- 1078 Allen-Diaz BH (1991) Water table and plant species relationships in
1079 Sierra Nevada meadows. *American Midland Naturalist* 126:30–43.
1080 <https://doi.org/10.2307/2426147>
- 1081 Baccei JS, McClaran MP, Kuhn TJ et al (2020) Multi-scale drivers of soil
1082 resistance predict vulnerability of seasonally wet meadows to trampling
1083 by pack stock animals in the Sierra Nevada, USA. *Ecol Process* 9. <https://doi.org/10.1186/s13717-020-00236-7>
- 1085 Baldocchi DD (2008) ‘Breathing’ of the terrestrial biosphere: lessons
1086 learned from a global network of carbon dioxide flux measurement
1087 systems. *Australian Journal of Botany* 56:1–26. <https://doi.org/10.1071/BT07151>
- 1089 Baldocchi DD (2014) Measuring fluxes of trace gases and energy between
1090 ecosystems and the atmosphere – the state and future of the
1091 eddy covariance method. *Global Change Biology* 20:3600–3609.
1092 <https://doi.org/10.1111/gcb.12649>
- 1093 Beer C, Ciais P, Reichstein M, Baldocchi DD, Law BE, Papale D,
1094 Soussana JF, Ammann C, Buchmann N, Frank D, Gianelle D,
1095 Janssens IA, Knohl A, Köstner B, Moors E, Roupsard O,
1096 Verbeeck H, Vesala T, Williams CA, Wohlfahrt G (2009)
1097 Temporal and among-site variability of inherent water use efficiency
1098 at the ecosystem level. *Global Biogeochemical Cycles* 23:GB2018.
1099 <https://doi.org/10.1029/2008GB003233>
- 1100 Blankinship JC, Hart SC (2014) Hydrological control of greenhouse gas
1101 fluxes in a sierra Nevada subalpine meadow. *Arctic Antarctic Alpine*
1102 *Res* 46:355–364. <https://doi.org/10.1657/1938-4246-46.2.355>
- 1103 Burba G (2013) Eddy covariance method for scientific, industrial, agricultural
1104 and regulatory applications: a field book on measuring ecosystem gas exchange and areal emission rates. LI-Cor Biosciences,
1105 Lincoln, USA, p 331
- 1107 Castellví F, Oliphant AJ (2017) Daytime sensible and latent heat flux
1108 estimates for a mountain meadow using in-situ slow-response measurements. *Agric Forest Meteorol* 236:135–144. <https://doi.org/10.1016/j.agrformet.2017.01.003>
- 1109 Davis J, Blesius L, Slocombe M, Maher S, Vasey M, Christian P, Lynch
1110 P (2020) Unpiloted aerial system (UAS)-supported biogeomorphic
1111 analysis of restored Sierra Nevada montane meadows. *Remote*
1112 *Sensing* 12:1828. <https://doi.org/10.3390/rs12111828>
- 1113 Dong G, Guo J, Chen J, Sun G, Gao S, Hu L, Wang Y (2011) Effects of
1114 spring drought on carbon sequestration, evapotranspiration and wa-
1115 ter use efficiency in the Songnen meadow steppe in Northeast
1116 China. *Ecohydrology* 4:211–224. <https://doi.org/10.1002/eco.200>
- 1117 Dugas WA, Heuer ML, Mayeux HS (1999) Carbon dioxide fluxes over
1118 bermudagrass, native prairie, and sorghum. *Agric Forest Meteorol*
1119 93:121–139. [https://doi.org/10.1016/S0168-1923\(98\)00118-X](https://doi.org/10.1016/S0168-1923(98)00118-X)
- 1120 Dwire KA, Kauffman JB, Baham JE (2006) Plant species distribution in
1121 relation to water-table depth and soil redox potential in montane
1122 riparian meadows. *Wetlands* 26:131–146. [https://doi.org/10.1672/0277-5212\(2006\)26\[131:PSDIRT\]2.0.CO;2](https://doi.org/10.1672/0277-5212(2006)26[131:PSDIRT]2.0.CO;2)
- 1123 Fites-Kaufman JA, Rundel P, Stephenson N, Weixelman DA (2007)
1124 Montane and subalpine vegetation of the Sierra Nevada and
1125 Cascade ranges. *Terrestrial Vegetation of California*, pp 456–501
- 1126 Flanagan LB, Wever LA, Carlson PJ (2002) Seasonal and interannual
1127 variation in carbon dioxide exchange and carbon balance in a north-
1128 ern temperate grassland. *Global Change Biology* 8:599–615. <https://doi.org/10.1046/j.1365-2486.2002.00491.x>
- 1129 Gilmanov TG, Soussana JF, Aires L, Allard V, Ammann C, Balzarolo M,
1130 Barcza Z, Bernhofer C, Campbell CL, Cernusca A, Cescatti A
1131 (2007) Partitioning European grassland net ecosystem CO₂ ex-
1132 change into gross primary productivity and ecosystem respiration
1133 using light response function analysis. *Agric Ecosystems Environ*
1134 121:93–120. <https://doi.org/10.1016/j.agee.2006.12.008>
- 1135 Gilmanov TG, Tieszen LL, Wylie BK, Flanagan LB, Frank AB,
1136 Haferkamp MR, Meyers TP, Morgan JA (2005) Integration of
1137 CO₂ flux and remotely-sensed data for primary production and eco-
1138 system respiration analyses in the northern Great Plains: potential
1139 for quantitative spatial extrapolation. *Glob Ecol Biogeography* 14:
1140 271–292. <https://doi.org/10.1111/j.1466-822X.2005.00151.x>
- 1141 Hamlet AF, Mote PW, Clark MP, Lettenmaier DP (2005) Effects of
1142 temperature and precipitation variability on snowpack trends in the
1143 western United States. *J Climatol* 18:4545–4561. <https://doi.org/10.1175/JCLI3538.1>
- 1144 Hammersmark CT, Rains MC, Mount JF (2008) Quantifying the hydro-
1145 logical effects of stream restoration in a montane meadow, northern
1146 California, USA. *River Res Appl* 24:735–753. <https://doi.org/10.1002/rra.1077>
- 1147 Haugo RD, Halpern CB (2007) Vegetation responses to conifer encroachment in a western Cascade meadow: a chronosequence approach. *Bot* 85:285–298. <https://doi.org/10.1139/B07-024>
- 1148 Hirano T (2005) Seasonal and diurnal variations in topsoil and subsoil
1149 respiration under snowpack in a temperate deciduous forest, global
1150 *Biogeochem. Cycles* 19:GB2011. <https://doi.org/10.1029/2004GB002259>
- 1151 Hsieh CI, Katul G, Chi TW (2000) An approximate analytical model for
1152 footprint estimation of scalar fluxes in thermally stratified atmo-
1153 spheric flows. *Adv Water Resour* 23:765–772. [https://doi.org/10.1016/S0309-1708\(99\)00042-1](https://doi.org/10.1016/S0309-1708(99)00042-1)
- 1154 Hutchinson R, Weisman A, Ronning K (2020) Yuba headwaters meadow
1155 restoration monitoring report. South Yuba River citizens league,
1156 California Department of Fish & wildlife ecosystem restoration pro-
1157 gram #P1496009, p 50
- 1158 Jerome E, Beckers Y, Bodson B, Heinesch C, Moureaux B, Aubinet M
1159 (2014) Impact of grazing on carbon dioxide exchanges in an inten-
1160 sively managed Belgian grassland. *Agric Ecosyst Environ* 194:7–16
- 1161 Kato T, Tang Y, Gu S, Cui X, Hirota M, Du M, Li Y, Zhao X, Oikawa T
1162 (2004) Carbon dioxide exchange between the atmosphere and an
1163
- 1164
- 1165
- 1166
- 1167
- 1168
- 1169
- 1170
- 1171
- 1172

- 1173 alpine meadow ecosystem on the Qinghai–Tibetan plateau, China.
 1174 Agric Forest Meteorol 124:121–134. <https://doi.org/10.1016/j.agrformet.2003.12.008> 1239
- 1175 Kattelmann, R, Embury M (1996) Riparian areas and wetlands. Sierra 1240
- 1176 Nevada Ecosystem Project, Final Report to Congress (Vol. 3) 1241
- 1177 Kayranli B, Scholz M, Mustafa A, Hedmark Å (2010) Carbon storage 1242
- 1178 and fluxes within freshwater wetlands: a critical review. Wetlands 30:111–124. <https://doi.org/10.1007/s13157-009-0003-4> 1243
- 1180 Knowles JF, Blanken PD, Williams MW (2016) Wet meadow ecosystems 1244
- 1181 contribute the majority of overwinter soil respiration from 1245
- 1182 snow-scoured alpine tundra. J Geophys Res Biogeosci 121:1118– 1246
- 1183 1130. <https://doi.org/10.1002/2015JG003081> 1247
- 1184 Knox SH, Sturtevant C, Matthes JH, Koteen L, Verfaillie J, Baldocchi D 1248
- 1185 (2015) Agricultural peatland restoration: effects of land-use change 1249
- 1186 on greenhouse gas (CO_2 and CH_4) fluxes in the Sacramento-san 1250
- 1187 Joaquin Delta. Glob Change Biol 21:750–765. <https://doi.org/10.1007/s13157-009-0003-4> 1251
- 1190 Kondolf GM, Kattelmann R, Embury M and Erman DC (1996) Status of 1252
- 1191 riparian habitat. Sierra Nevada ecosystem project: final report to 1253
- 1192 congress. Center for Water Wildlands Research. University of 1254
- 1193 California, Davis. (Vol. 2, 1009–1030) 1255
- 1194 Lee X, Massman W and Law B (2004) Handbook of micrometeorology: 1256
- 1195 a guide for surface flux measurement and analysis (Vol. 29). 1257
- 1196 Springer Science & Business Media 1258
- 1197 Loheide SP, Deitchman RS, Cooper DJ, Wolf EC, Hammersmark CT, 1259
- 1198 Lundquist JD (2009) A framework for understanding the 1260
- 1199 hydroecology of impacted wet meadows in the Sierra Nevada and 1261
- 1200 Cascade ranges, California, USA. Hydrogeol J 17:229–246. <https://doi.org/10.1007/s10040-008-0380-4> 1262
- 1201 Loheide SP, Gorelick SM (2007) Riparian hydroecology: a coupled 1263
- 1202 model of the observed interactions between groundwater flow and 1264
- 1203 meadow vegetation patterning. Water Resour Res 43. <https://doi.org/10.1029/2006WR005233> 1265
- 1204 Lowry CS, Loheide SP, Moore CE, Lundquist JD (2011) Groundwater 1266
- 1205 controls on vegetation composition and patterning in mountain 1267
- 1206 meadows. Water Resour Res 47. <https://doi.org/10.1029/2010WR010086> 1268
- 1207 Lund M, Lafleur PM, Roulet NT, Lindroth A, Christensen TR, Aurela M, 1269
- 1208 Chojnicki BH, Flanagan LB, Humphreys ER, Laurila T, Oechel WC 1270
- 1209 (2010) Variability in exchange of CO_2 across 12 northern peatland 1271
- 1210 and tundra sites. Glob Change Biol 16:2436–2448. <https://doi.org/10.1111/j.1365-2486.2009.02104.x> 1272
- 1211 Ma S, Baldocchi DD, Xu L, Hehn T (2007) Inter-annual variability in 1273
- 1212 carbon dioxide exchange of an oak/grass savanna and open grass- 1274
- 1213 land in California. Agric Forest Meteorol 147:157–171. <https://doi.org/10.1016/j.agrformet.2007.07.008> 1275
- 1214 Maher SC (2015) Bio-micrometeorology of a Sierra Nevada Montane 1276
- 1215 Meadow. Masters Thesis, San Francisco State University 1277
- 1216 Massman WJ, Lee X (2002) Eddy covariance flux corrections and 1278
- 1217 uncertainties in long-term studies of carbon and energy exchanges. Agric 1279
- 1218 Forest Meteorol 113(1–4):121–144. [https://doi.org/10.1016/S0168-1923\(02\)00105-3](https://doi.org/10.1016/S0168-1923(02)00105-3) 1280
- 1219 Norton JB, Jungst LJ, Norton U, Olsen HR, Tate KW, Horwath WR 1281
- 1220 (2011) Soil carbon and nitrogen storage in upper montane riparian 1282
- 1221 meadows. Ecosystems 14:1217–1231. <https://doi.org/10.1007/s10021-011-9477-z> 1283
- 1222 Oliphant AJ (2012) Terrestrial ecosystem-atmosphere exchange of CO_2 , 1284
- 1223 water and energy from FLUXNET; review and meta-analysis of a 1285
- 1224 global in-situ observatory. Geography Compass 6:689–705. <https://doi.org/10.1111/gec3.12009> 1286
- 1225 Oliphant AJ, Dragoni DD, Deng B, Grimmond CSB, Schmid HP, Scott 1287
- 1226 SL (2011) The role of sky conditions on gross primary production in 1288
- 1227 a mixed deciduous forest. Agric Forest Meteorol 151:781–791. 1289
- 1228 <https://doi.org/10.1016/j.agrformet.2011.01.005> 1290
- 1229 Papale D, Reichstein M, Aubinet M, Canfora E, Bernhofer C, Kutsch W, 1291
- 1230 Longdoz B, Rambal S, Valentini R, Vesala T, Yakir D (2006) 1292
- 1231 Towards a standardized processing of net ecosystem exchange measured 1293
- 1232 with eddy covariance technique: algorithms and uncertainty estimation. Biogeosciences 3:571–583 <https://hal.archives-ouvertes.fr/hal-00330317> 1294
- 1233 Plumas Corporation (2020) Mountain meadows restoration project at 1295
- 1234 Greenville Creek and upper Goodrich and effects on greenhouse 1296
- 1235 gases, wetlands restoration for greenhouse gas reduction, final report 1297
- 1236 CDFW Grant agreement P1496002 01. Center for Watershed 1298
- 1237 Sciences, University of California, Davis 1299
- 1238 Ponton S, Flanagan LB, Alstad KP, Johnson BG, Morgenstern K, Kljun N, 1300
- 1239 Black TA, Barr AG (2006) Comparison of ecosystem water-use efficiency among Douglas-fir forest, aspen forest and grassland using eddy covariance and carbon isotope techniques. Glob Change Biol 12:294–310. <https://doi.org/10.1111/j.1365-2486.2005.01103.x> 1301
- 1240 Pope KL, Montoya DS, Brownlee JN, Dierks J, Lisle TE (2015) Habitat 1302
- 1241 conditions of montane meadows associated with restored and unre- 1303
- 1242 stored stream channels of California. Ecol Restoration 33(1):61–73. 1304
- 1243 <https://doi.org/10.3368/er.33.1.61> 1305
- 1244 Purdy SE, Moyle PB (2006) Mountain meadows of the Sierra Nevada. 1306
- 1245 Center for Watershed Sciences, University of California, Davis 1307
- 1246 Ratliff RD (1982) A meadow site classification for the Sierra Nevada, 1308
- 1247 California. USDA Forest Service General Technical Report PSW- 1309
- 1248 60:16. <https://doi.org/10.2737/PSW-GTR-60> 1310
- 1249 Ratliff RD (1985) Meadows in the Sierra Nevada of California: state of 1311
- 1250 knowledge. USDA Forest Service general technical report PSW-GTR-84, 52. <https://doi.org/10.2737/PSW-GTR-84> 1312
- 1251 Reed CC, Merrill AG, Drew WM, Christman B, Hutchinson RA, Kessey L, 1313 Odell M, Swanson S, Verburg PSJ, Wilcox J, Hart SC, Sullivan BW (2020) Montane meadows: a soil carbon sink or source? 1314
- 1252 Ecosystems. <https://doi.org/10.1007/s10021-020-00572-x> 1315
- 1253 Reed CC, Winters JM, Hart SC, Hutchinson R, Chandler M, Venicitz G, 1316 Sullivan BW (2018) Building flux capacity: citizen scientists increase 1317 resolution of soil greenhouse gas fluxes. PLoS One 13: e0198997. <https://doi.org/10.1371/journal.pone.0198997> 1318
- 1254 Reichstein M, Falge E, Baldocchi D, Papale D, Aubinet M, Berbigier P, 1319 Bernhofer C, Buchmann N, Gilmanov T, Granier A, Grünwald T (2005) 1320
- 1255 On the separation of net ecosystem exchange into assimilation and 1321 ecosystem respiration: review and improved algorithm. Glob Change Biol 11:1424–1439. <https://doi.org/10.1111/j.1365-2486.2005.001002.x> 1322
- 1256 Roche LM, O'Green AT, Latimer AM, Eastburn DJ (2014) Montane 1323
- 1257 meadow hydropedology, plant community, and herbivore dynamics. Ecosphere 5:1–16. <https://doi.org/10.1890/ES14-00173.1> 1324
- 1258 Scott RL, Hamerlynck EP, Jenerette GD, Moran MS, Barron-Gafford GA (2010) Carbon dioxide exchange in a semidesert grassland through 1325
- 1259 drought-induced vegetation change. J Geophys Res 115(G3). 1326
- 1260 <https://doi.org/10.1029/2010JG001348> 1327
- 1261 Sommerfeld R, Mosier A, Musselman R (1993) CO_2 , CH_4 and N_2O flux 1328
- 1262 through a Wyoming snowpack and implications for global budgets. 1329
- 1263 Nature 361:140–142. <https://doi.org/10.1038/361140a0> 1330
- 1264 Soussana JF, Allard V, Pilegaard K, Ambus P, Amman C, Campbell C, 1331 Ceschia E, Clifton-Brown J, Czobél SZ, Domingues R, Flechard C (2007) 1332 Full accounting of the greenhouse gas (CO_2 , N_2O , CH_4) budget of nine European grassland sites. Agric Ecosyst Environ 121:121–134. <https://doi.org/10.1016/j.agee.2006.12.022> 1333
- 1265 Stewart IT, Cayan DR, Dettling MD (2005) Changes toward earlier 1334
- 1266 streamflow timing across western North America. J Climatol 18: 1335
- 1267 1136–1155. <https://doi.org/10.1175/JCLI3321.1> 1336
- 1268 Stoy PC, Mauder M, Foken T, Marcolla B, Boegh E, Ibrom A, Arain MA, 1337 Arneth A, Aurela M, Bernhofer C, Cescatti A (2013) A data- 1338 driven analysis of energy balance closure across FLUXNET research 1339
- 1269 sites: the role of landscape scale heterogeneity. Agric Forest Meteorol 171:137–152. <https://doi.org/10.1016/j.agrformet.2012.11.004> 1340

- 1304 Tofastrud M, Hesse A, Rekdal Y, Zimmermann B (2020) Weight gain of
 1305 free-ranging beef cattle grazing in the boreal forest of South-Eastern
 1306 Norway. *Livestock Sci* 233:103955. <https://doi.org/10.1016/j.livsci.2020.103955> 1326
- 1307 Viers JH, Purdy SE, Peek RA, Fryjoff-Hung A, Santos NR, Katz JV,
 1308 Emmons JD, Dolan DV, Yarnell SM (2013) Montane Meadows
 1309 In The Sierra Nevada: Changing Hydroclimatic Conditions and
 1310 Concepts for Vulnerability Assessment. Centerfor Watershed
 1311 Sciences Technical Report (CWS-2013-01), University of
 1312 California, Davis, p 63 1328
- 1313 Viers JH, Rheinheimer DE (2011) Freshwater conservation options for a
 1314 changing climate in California's Sierra Nevada. *Marine Freshwater*
 1315 Res 62:266–278. <https://doi.org/10.1071/MF09286> 1329
- 1316 Weixelman DA, Hill B, Cooper DJ, Berlow EL, Viers JH, Purdy SE,
 1317 Merrill AG, Gross SE (2011) A field key to meadow hydrogeomorphic
 1318 types for the Sierra Nevada and southern Cascade ranges in
 1319 California. US Forest Service, Pacific Southwest Region, Vallejo,
 1320 California, USA 1330
- 1321 Wilson K, Goldstein A, Falge E, Aubinet M, Baldocchi D, Berbigier P,
 1322 Bernhofer C, Ceulemans R, Dolman H, Field C, Grelle A (2002)
 1323 Energy balance closure at FLUXNET sites. *Agric Forest Meteorol*
 1324 113:223–243. [https://doi.org/10.1016/S0168-1923\(02\)00109-0](https://doi.org/10.1016/S0168-1923(02)00109-0) 1325
- 1325 Wohlfahrt G, Hammerle A, Haslwanter A, Bahn M, Tappeiner U,
 1326 Cernusca A (2008) Seasonal and inter-annual variability of the net
 1327 ecosystem CO₂ exchange of a temperate mountain grassland: effects
 1328 of weather and management. *J Geophys Res* 113(D8). <https://doi.org/10.1029/2007JD009286> 1329
- 1329 WRCC (Western Regional Climate Center) (2020) Data portal Accessed
 1330 20 Nov 2020. Retrieved from <https://wrcc.dri.edu/cgi-bin/cliMAIN.pl?ca1018> 1330
- 1330 Xu L, Baldocchi DD (2004) Seasonal variation in carbon dioxide ex-
 1331 change over a Mediterranean annual grassland in California. *Agric*
 1332 *Forest Meteorol* 123(1–2):79–96. <https://doi.org/10.1016/j.agrformet.2003.10.004> 1333
- 1331 Zegelin SJ, White I, Russell G (1992) In: Topp GC, Reynolds WD, Green
 1332 RE (eds) A critique of the time domain Reflectometry technique for
 1333 determining Field soil-water content. In advances in measurement of
 1334 soil physical properties: bringing theory into practice. <https://doi.org/10.2136/sssaspecpub30.c10> 1334
- 1334 **Publisher's Note** Springer Nature remains neutral with regard to jurisdictional
 1335 claims in published maps and institutional affiliations. 1335
- 1335
- 1336
- 1337
- 1338
- 1339
- 1340
- 1341
- 1342
- 1343
- 1344

AUTHOR QUERIES

AUTHOR PLEASE ANSWER ALL QUERIES.

- Q1. Please check if the affiliation is presented correctly.
- Q2. Please check Eq. 4 citation.
- Q3. Availability of data and material was changed to Data availability. Please check if appropriate.

UNCORRECTED PROOF